CHAPTER 2

Chemical Wet Texturing Process of Electrodes

Surface modification of ZnO photoelectrodes is an expected for improving porous structure which is a good structure for dye adsorption. The dye adsorption is an important factor that direct affect to current density and power conversion efficiency. A chemical wet texturing process is presented in this chapter to modify surface of ZnO photoelectrodes for achieving dye adsorption as mainly. The chemical wet texturing process means a direct immersion of ZnO photoelectrodes into the chemical texturing solution. This process is a typical popular technique due to simplicity and short-time process. Moreover, there are a lot of chemicals for using as texturing solutions such as HCl, HNO_3, H_2SO_4, NaOH, KOH, HP_4O_3, P_2SO_4 and Na_2SO_4 [34,52,55,56].

In this chapter, the surface modification of ZnO photoelectrodes using chemical wet texturing process of base and acid solutions are investigated. ZnO is well known that can solute in base and acid solution with different solubility (higher solubility in acid than base). Thus, texturing time is varied to optimize an appropriate texturing of ZnO surface for both base and acid solution. A power conversion efficiency enhancement of DSSCs based on texturing ZnO photoelectrodes are discusses. Experimental sections are separated in two sections consisted of one- and two-step texturing process. The one-step texturing process is introduced as preliminary study for understanding the effects of base and acid solutions on the ZnO photoelectrodes properties and photovoltaic characteristics. The two-step texturing process is used to sequential modify ZnO photoelectrodes step by step for improving optimal surface according to the roles of each solutions.

2.1 One-step texturing process

The one-step texturing process is mentioned on characteristic effects of base and acid solutions on ZnO photoelectrodes to understand the roles of base and acid solutions for texturing ZnO films. Moreover, the effects of base and acid solutions on photovoltaic characteristics will be deeply studied. For experimental detail, fluorine-doped tin oxide (FTO) substrate (purchased from Sigma-Aldrich, resistivity ~ 7 Ω/sq) was sonicated with distilled water, acetone and ethanol for 15 min each, respectively. An aqueous solution of polyethylene glycol (PEG) was prepared at 10 wt.% in distilled water and stirring at room temperature for 6 h to form a clear solution. 5 g of ZnO nanoparticles was added in 12 mL of the PEG solution. The mixture was stirred at room temperature for 24 h to form ZnO paste. Next, the paste was coated onto the cleaned FTO substrate using a doctor blade technique [57] and immediately annealed at 400 ^{o}C for 1 h for evaporating PEG and form a ZnO films. After cooling down, two kinds of texturing solutions were carried out to texture ZnO surface included base and acid solutions. A dilute NH_4OH with concentration of 5% in distilled water represents the base solution and a mixtures of HCl:HNO_3:distilled water with volumetric ratio of 0.3:0.7:0.44, respectively, represent the acid solution. A direct immersion of ZnO films was performed in a vertical direction into a texturing bath. The texturing films were maintained in the base and acid solutions for texturing time of 1-3 min and 10-30 s, respectively. After the texturing process, the films were rinsed with distilled water for several times to stop reaction and remove residuals. Finally, the films were annealed at 120 ^{o}C for 30 min to evaporate humidity.

2.1.1 Morphology

Morphologies of the texturing ZnO films were observed by field-emission scanning electron microscopy (FE-SEM, JEOL JSM-6335F) operating at a voltage of 15.0 kV [28] as can be seen in Figure 2.1. The FE-SEM images show a change in morphology, and porous structures are observed after the texturing process.

From the FE-SEM images, a short texturing time of 1 min is not enough to remove numerous aggregate particles from the ZnO surface which can be observed both of fine pores and aggregate particles at the surface as shown in Figure 2.1(b). This result

is due to a slow reaction rate of base solution. On the other hand, a texturing time of 3 min is an over texturing time for texturing ZnO surface which can be observed a rough porous structure as shown in Figure 2.1(d). The texturing time of 2 min shows an optimization of texturing time for balancing between aggregate particles removal and pore formation. Therefore, an appropriate porous structures are formed which is shown in Figure 2.1(c).

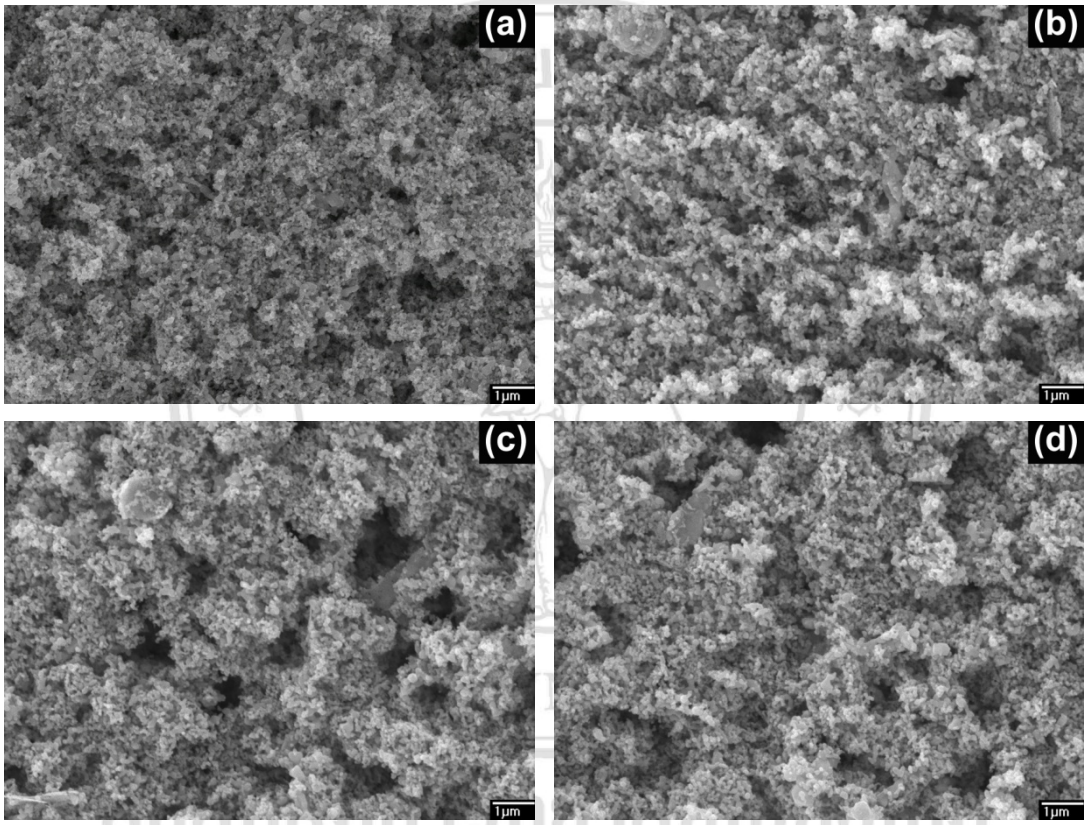

Figure 2.1 Morphology of base texturing ZnO films for texturing time of (a) 0 min, (b) 1 min, (c) 2 min and (d) 3 min.

A formation of porous structures is due to chemical reactions which can be represented according to the equation (2.1)-(2.4) [58,59].

$$NH_4OH \rightarrow NH_4^+ + OH^- \quad (2.1)$$

$$NH_4^+ + H_2O \leftrightarrow NH_3 + H_3O^+ \quad (2.2)$$

$$ZnO + H_3O^+ \rightarrow Zn^{2+} + 3H_2O \quad (2.3)$$

$$Zn^{2+} + 2OH^- \rightarrow Zn(OH)_2 \quad (2.4)$$

After the dissolution of NH_4OH in water, hydronium ion (H_3O^+) is formed according to the equation (2.1)-(2.2). This is a spontaneous reaction for decreasing internal energy of NH_4OH. During the immersion of ZnO films into the solutions, the H_3O^+ reacts with electrons at oxygen site of ZnO atom. After the H_3O^+ reaction, Zn^{2+} is leaved at the surface and small pores are formed for short texturing time. This reaction results in formation of fine porous structures. For long texturing time, a hydroxide ion (OH^-) is continuous reacts with the leaved Zn^{2+} to form $Zn(OH)_2$ and results a removed Zn^{2+} (see equation (2.4)). After the ZnO particles are completely removed from an outer surface layer, large pore is formed which is correlated to a rough porous structures. Therefore, the chemical reaction can creates both of fine and rough porous structures by varying the texturing time.

To calculate the texturing rate, thickness of texturing ZnO films for various texturing times was measured. Figure 2.2 shows cross-sectional FE-SEM images of texturing films, the thickness is directly measured using image-J software. The maximum thickness is typically observed for the non-texturing films. After texturing process, the thickness decreases with texturing time as listed in Table 2.1. The decrease in thickness can be briefly described by a continuous removal of aggregate particles during the chemical reaction. According to the measured thickness results, the texturing rate is fitted as linear relation between thickness and texturing time. An estimated texturing rate of ZnO films is about 1.49 μm/min.

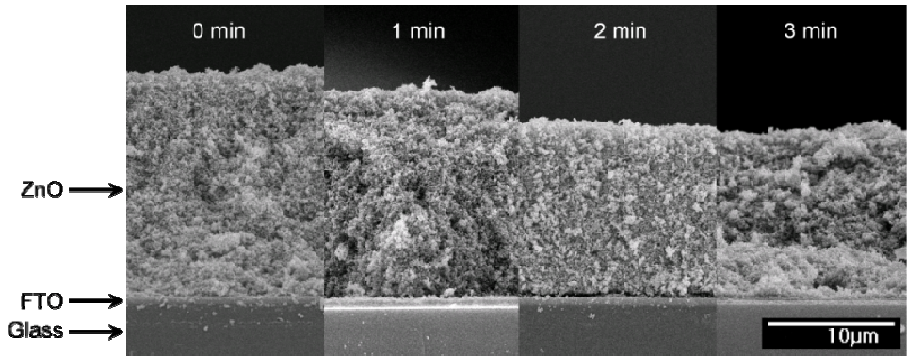

Figure 2.2 Cross-sectional FE-SEM images of base texturing films.

Table 2.1 Thickness of base texturing films.

Texturing time (min)	Thickness (μm)			
	Average	SD	Max	Min
0	18.02	0.28	18.40	17.51
1	16.20	0.31	16.77	15.73
2	14.01	0.60	15.14	13.28
3	13.79	0.44	14.76	12.91

2.1.2 Specific surface area

Specific surface area (SSA) was measured by the Brunauer–Emmett–Teller (BET, Quantachrome Autosorb 1 MP) method using N_2 gas [60] to understand effects of specific surface area on DSSCs performance. The measured specific surface area is listed in Table 2.2. The specific surface area of the texturing films rapidly increases over two times in comparison to the non-texturing films. The specific surface area reached maximum value of 5.71 m^2/g for texturing time of 1 min, and slightly decreased for longer texturing time. The result suggests that a simple modification of ZnO films by chemical wet texturing process of base solutions can be effectively improved specific surface area.

2.1.3 Reflectance

Figure 2.3 shows reflectance of texturing films measured using UV-Vis-NIR spectroscopy (Varian cary 50, wavelength range 190-1100 nm). Average reflectance in range of 400-700 nm are 0.1778%, 0.1783%, 0.1766% and 0.1824% for texturing time of 0, 1, 2 and 3 min, respectively. There is not much difference for all the films, it indicates a negligibly changed in optical property of the films after the texturing process.

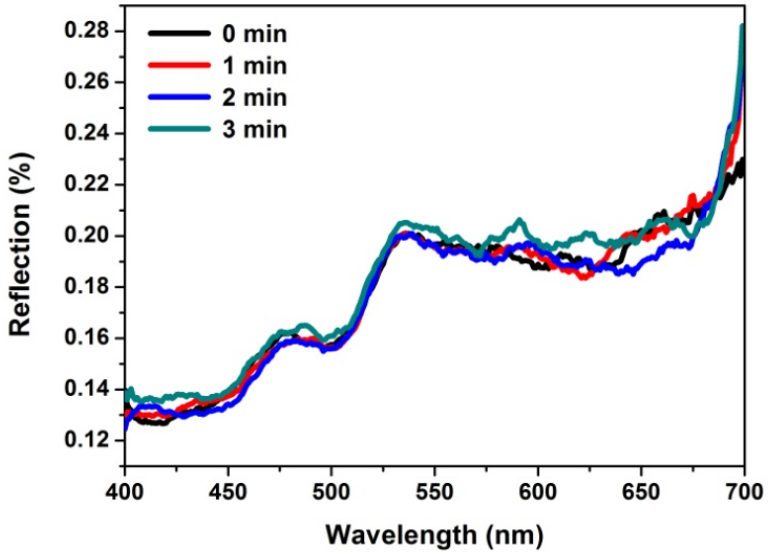

Figure 2.3 Reflectance of base texturing films.

2.1.4 Dye adsorption

Dye adsorption was measured using UV-Vis-NIR spectroscopy (Varian cary 50, wavelength range 190-1100 nm). Adsorbed dye molecules were extracted by an immersion of dye-sensitized photoelectrodes in a NaOH solution with concentration of 0.1 M dissolved in an equal volume mixture of water and ethanol [56]. Measured dye adsorption is shown in Figure 2.4. Eosin-Y (EY) and Di-tetrabutylammonium cis-bis(isothiocyanato) bis(2,2′-bipyridyl-4,4′-dicarboxylato) ruthenium(II) (N719) sensitizers are used to parallel investigate the dye adsorption effect on texturing films. The extracted adsorbed dye from the texturing films for texturing time of 2 min shows a maximum intensity peaks for both of EY and N719 sensitizers, indicating a maximum

amount of dye adsorption. The amount of dye adsorption was evaluated by the Beer-Lambert law, and listed in Table 2.2.

$$A = c\varepsilon L \tag{2.5}$$

A is absorbance, c is dye concentration, ε is molar extinction coefficient (ε = 89,560 $M^{-1}cm^{-1}$ at wavelength of 532 nm for EY [61] and ε = 14,100 $M^{-1}cm^{-1}$ at wavelength of 515 nm for N719 [62,63]) and L is length of dye solution (1 cm). The dye adsorption increases as increasing texturing time for initially. It shows a maximum intensity for texturing time of 2 min, and decreases for texturing time of 3 min. From the dye adsorption result, it can be implied that the texturing time of 2 min for base solution texturing process is an optimal condition for achieving dye adsorption which agree with the specific surface area result. An increment of dye adsorption is considered as a major factor for enhancing power conversion efficiency of ZnO DSSCs because light harvesting efficiency at a particular wavelength, ϕ_{LHE}, is directly changed corresponds to dye absorbance according to the relation [30,46],

$$\emptyset_{LHE} = (1 - R)(1 - 10^{-A}) \tag{2.6}$$

The R and A are reflectance and absorbance, respectively. From the reflectance result, the average reflectance is very close for all the films. It can be considered that the light harvesting efficiency is a typical correlation with the dye adsorption.

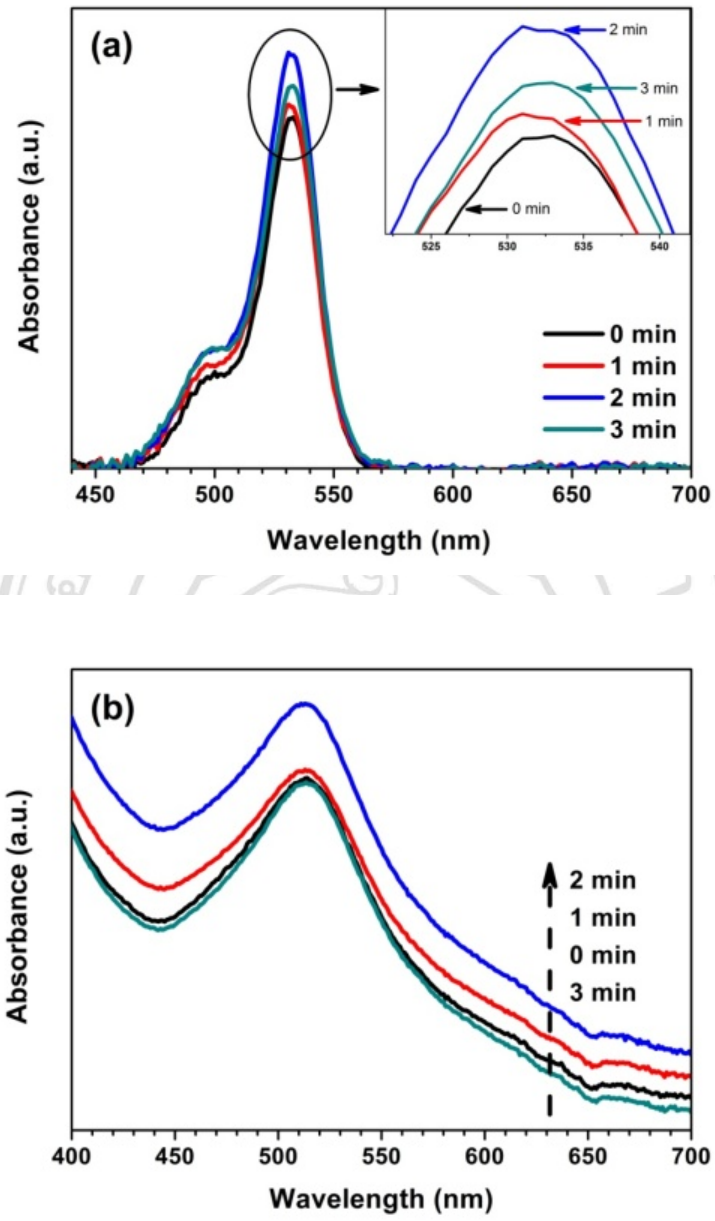

Figure 2.4 Dye adsorption of base texturing films for (a) EY sensitizer and (b) N719 sensitizer.

Table 2.2 Specific surface area and dye adsorption of base texturing films.

Texturing time (min)	Specific surface area (m^2/g)	Dye adsorption (10^{-9} mol/cm^2)	
		EY	N719
0	2.52	9.33	43.67
1	5.71	9.65	44.85
2	5.30	11.04	53.03
3	4.29	10.19	43.10

2.1.5 Photovoltaic characteristics

After the surface modification via chemical wet texturing process, a dye adsorption process was performed by a direct immersion of texturing ZnO films in dye solution at room temperature under a dark condition to form an adsorbed-dye ZnO photoelectrodes. The adsorption process is separated as 4 steps for optimizing amount of dye adsorption as shown in Figure 2.5 [64,65]. The first step is an immersion of films into a bath of dye solution for adsorption. Next, a desorption step is used for desorbing aggregate dye from the surface by immersing the films into ethanol. After the desorption, the films were repeating immersed in dye solution for re-adsorption. Finally, the films were rinsed with ethanol and dried in normal ambient. All of the steps were kept a constant period of 1 h. Two kinds of dye solutions were used in this work included EY and N719. The EY solution was prepared by dissolving EY with concentration of 0.6 mM in absolute ethanol and stirring for 1 h to form a pink solution. The N719 solution was prepared by dissolving N719 with a concentration of 0.3 mM in a mixing solvent of acetone nitride and tert-butanol with an equal volume ratio, and stirring for 1 h to form a dark-red solution. Both of the solutions were stocked under the dark condition. A counterelectrode was prepared by dropping a H_2PtCl_6 solution on FTO substrate and sintered at 550 ^oC for 1 h to form Pt counterelectrode. The H_2PtCl_6 solution was prepared by dissolving H_2PtCl_6 with concentration of 0.05 mM into a mixed solvent of acetone and propanol with a volume ratio of 9:1, respectively. The

mixture was sonicated at room temperature for 1 h to form a dark-brown H_2PtCl_6 solution.

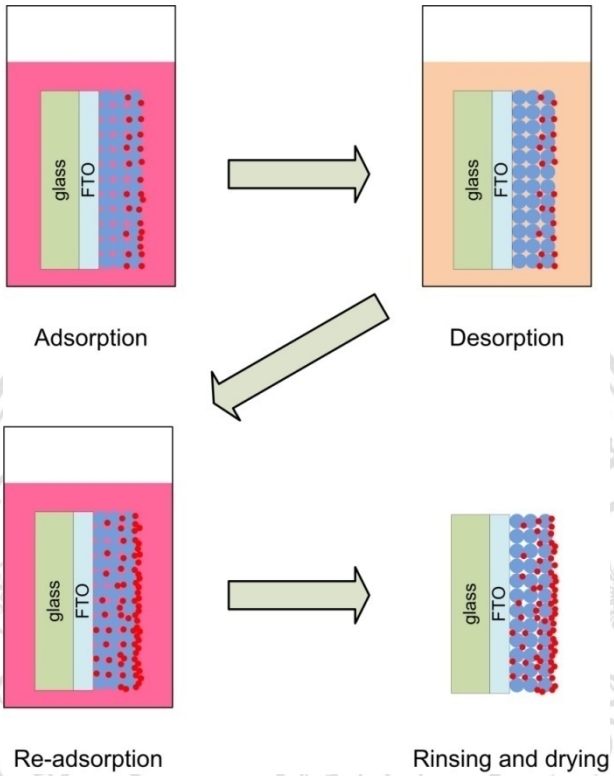

Figure 2.5 Flowing diagram of dye adsorption process.

An electrolyte solution for the EY was prepared by dissolving LiI and I_2 with concentration of 0.2 and 0.02 M in propylene carbonate. For the N719, LiI, I_2 and DMPII were dissolved in acetone nitride with concentration of 0.3, 0.03 and 0.3 M, respectively. The mixing solutions were performed by stirring at room temperature for 1 h, and stocked in a dark condition. A DSSC was fabricated by sandwiching the photoelectrode, counterelectrode, polymer film, and electrolyte. A fabrication detail, the counterelectrode was sequentially covered by a polymer film and the photoelectrode, respectively. Next, hot air was flowed at the counterelectrode for melting the polymer. After the fabrication, the electrolyte was injected into the gap between the both electrodes and the photovoltaic characteristics were immediately measured under standard condition with a simulation of solar light intensity of 100 mW/cm^2 (AM1.5).

Current density – voltage (J-V) characteristics were measured under standard condition (AM1.5) as shown in Figure 2.6. In addition, calculated photovoltaic parameters include short-current density (J_{sc}), open-circuit voltage (V_{oc}), fill factor (FF) and power conversion efficiency (PCE) are summarized in Table 2.3. It was found that the J_{sc} increased and reached maximum values of 4.77 mA/cm^2 and 7.15 mA/cm^2 for EY and N719 respectively, at the texturing time of 2 min. The change in J_{sc} shows a significant correlation with PCE for both of EY and N719. Meanwhile, the V_{oc} shows small changed. Typically, V_{oc} is a well known that strong depending on a difference in an internal energy level between Fermi level of FTO and redox potential of electrolyte [66]. In this work, FTO and electrolyte are controlled. Thus, the result indicating that texturing solutions is not affect on the internal energy level. It can be concluded that the texturing solutions only react with aggregate particles and remove the particles from the surface.

From the result, the J_{sc} is considered as a major factor for enhancing PCE which is related with amount of dye adsorption as shown in Figure 2.7. It is clearly observed that J_{sc} increases as increasing amount of dye adsorption. It is attributed that J_{sc} is governed by the amount of dye adsorption [67] which can be seen in term of light harvesting efficiency,Φ_{LHE}, according the relation [66],

$$J_{sc} = \Phi_{LHE}\, \Phi_G\, \Phi_C \tag{2.7}$$

Φ_G is electron generation efficiency of dye molecule under excitation condition and Φ_C is charge collection efficiency of ZnO.

Table 2.3 Photovoltaic parameters of DSSCs fabricated with base texturing films.

Sensitizer	Texturing time (min)	J_{sc} (mA/cm^2)	V_{oc} (V)	FF	PCE (%)
EY	0	3.48 ± 0.08	0.45 ± 0.01	0.42 ± 0.01	0.67 ± 0.02
	1	4.22 ± 0.06	0.45 ± 0.01	0.37 ± 0.03	0.70 ± 0.05
	2	4.77 ± 0.47	0.44 ± 0.01	0.39 ± 0.04	0.80 ± 0.02
	3	4.35 ± 0.30	0.44 ± 0.01	0.35 ± 0.01	0.66 ± 0.05
N719	0	6.61 ± 0.26	0.57 ± 0.01	0.48 ± 0.02	1.80 ± 0.01
	1	6.87 ± 0.25	0.56 ± 0.01	0.47 ± 0.01	1.81 ± 0.01
	2	7.15 ± 0.32	0.57 ± 0.01	0.49 ± 0.02	2.00 ± 0.01
	3	6.96 ± 0.13	0.57 ± 0.01	0.47 ± 0.01	1.85 ± 0.08

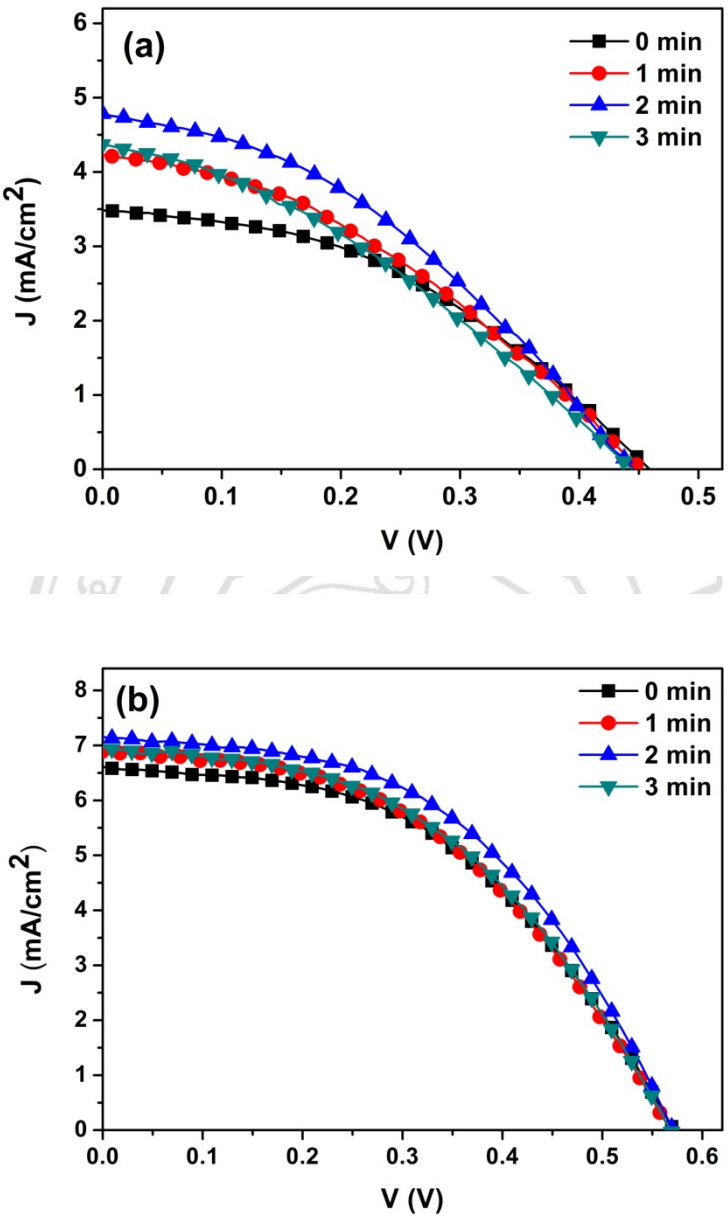

Figure 2.6 Photovoltaic characteristics of DSSCs fabricated with base texturing films for (a) EY sensitizer and (b) N719 sensitizer.

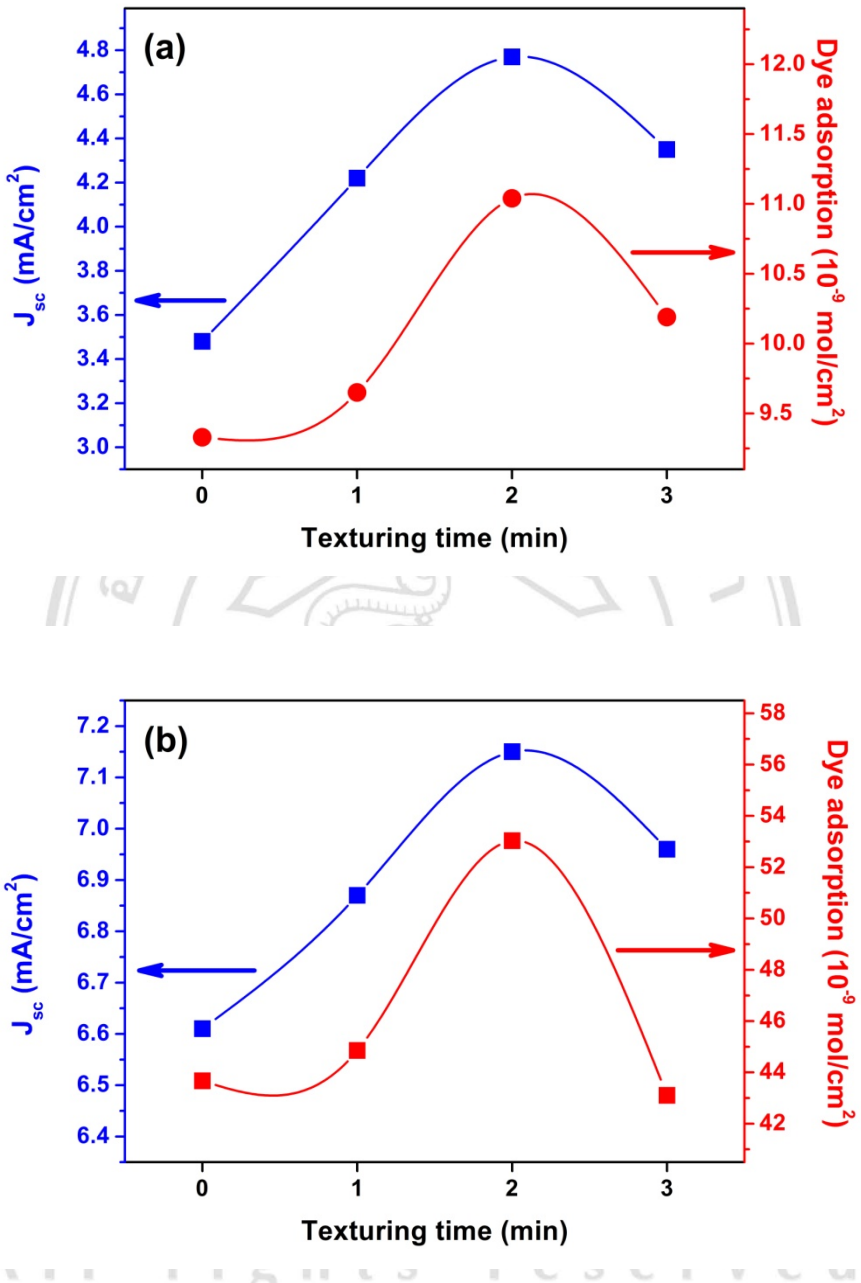

Figure 2.7 Plots of J_{sc} and dye adsorption for (a) EY sensitizer and (b) N719 sensitizer.

2.1.6 Electrochemical impedance spectroscopy analysis

An internal recombination of electron in fabricated DSSCs was analyzed from electrochemical impedance spectroscopy (EIS) with frequency range of 10 kHz to 1 Hz and AC amplitude of 20 mV [57]. The EIS was measured under dark condition with forward bias voltage of -0.7 V to maintain a steady-state condition. Internal parameters were fitted using Z-view software under equivalent circuits according to the Figure 2.8 [46]. Three main internal resistances of R_s, R_{ct1} and R_{ct2} corresponds to series resistance, charge transfer resistance at electrolyte/counterelectrode interfaces, and charge transfer resistance at ZnO/dye/electrolyte interfaces, respectively [68]. Constant phase element (CPE) is used for smoothing the fitted curve. Figure 2.9 shows a Nyquist plot of measured EIS and fitting parameters are summarized in Table 2.4. In this work, R_{ct2} represents a recombination resistance (R_{rec}) at the photoelectrodes by measuring under dark condition [24]. All of texturing films based DSSCs exhibit larger R_{ct2} compare to the non-texturing films. This result indicates a lower electron recombination at the ZnO/dye/electrolyte interfaces because lower number of electrons (n) involve in the reaction at the interfaces which can be described in equation (2.8) [69],

$$R_{ct} = \frac{R\,T}{n\,F\,J_0} \tag{2.8}$$

R, T, F and J_0 represent gas constant (8.31 J/mol.K), absolute temperature, Faraday's constant (9.65×10^4 C/mol) and exchange current density, respectively. The reduction of electron recombination results a reduction of J_0 which lead an increment of J_{sc}.

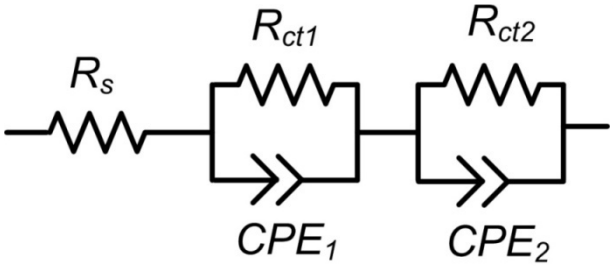

Figure 2.8 An equivalent circuits of DSSCs for recombination analysis.

Small change in R_s can be described by a change of surface resistance of FTO due to chemical reaction during the texturing process. R_{ct1} change is due to a non-uniform of Pt counterelectrodes.

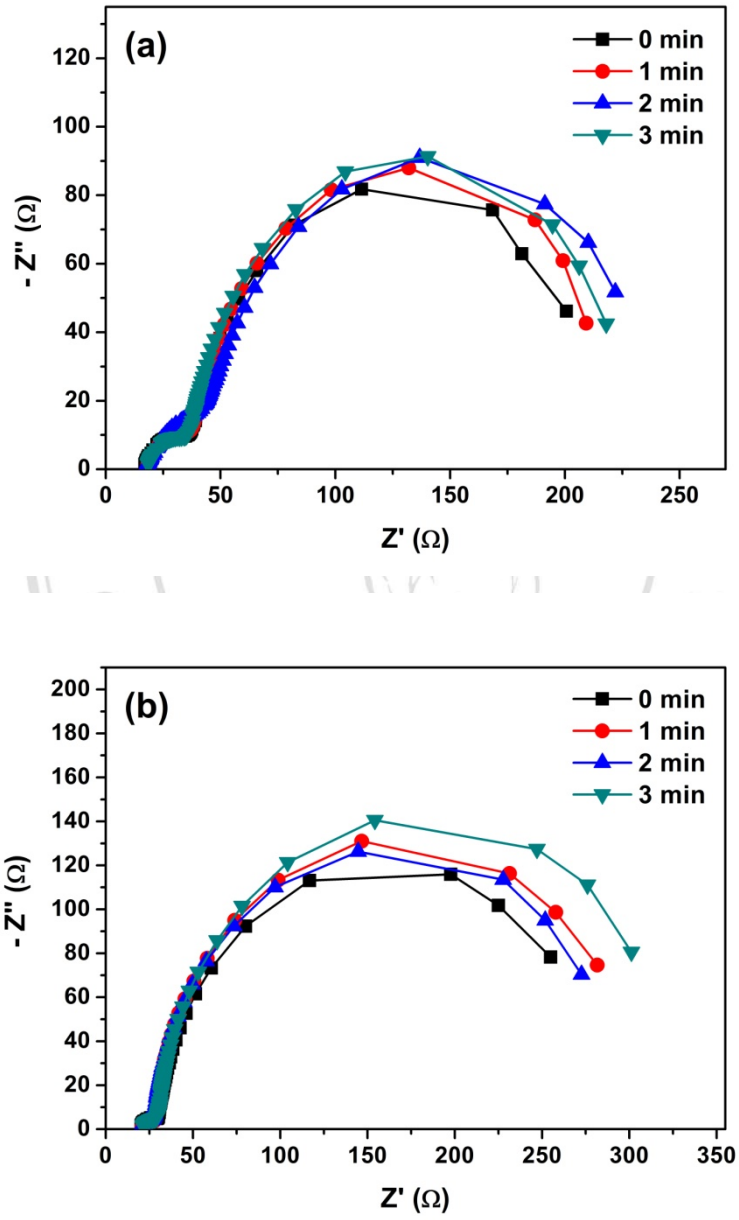

Figure 2.9 Nyquist plots of DSSCs fabricated with base texturing films for (a) EY sensitizer and (b) N719 sensitizer.

Electron life time (τ), which means duration of electron movement in conduction band of ZnO before recombine with oxidized dye or electrolyte [70], was calculated from the equation [17,67],

$$\tau = \frac{1}{2\,\pi f_{peak}} \tag{2.9}$$

The f_{peak} is the frequency at the maximum peak from the Bode phase plots as shown in Figure 2.10. The calculated electron life time is in order of milliseconds indicating a recombination process of electron from conduction ban of ZnO with electrolyte is dominance. In addition, small change in electron life time indicates an unchanged duration of electron movement in conduction band of ZnO but the increased R_{ct1} was observed. The results imply an improvement of electron transport in the fabricated cells. However, the internal effect is not a significant factor for enhancing PCE in comparison to the effects of dye adsorption. These results are observed in similar trend for both of EY and N719 sensitizers.

Table 2.4 EIS parameters of DSSCs fabricated with base texturing films.

Sensitizer	**Texturing time (min)**	**R_s (Ω)**	**R_{ct1} (Ω)**	**R_{ct2} (Ω)**	**f_{peak} (Hz)**	**τ (ms)**
EY	0	16.8	22.3	169.6	8	19.9
	1	18.1	21.8	178.7	10	15.9
	2	17.8	32.2	179.9	8	19.9
	3	18.3	20.1	185.9	10	15.9
N719	0	20.1	10.7	243.6	8	19.9
	1	21.7	7.3	267.5	10	15.9
	2	20.5	8.0	256.3	12	13.3
	3	21.2	9.5	287.7	12	13.3

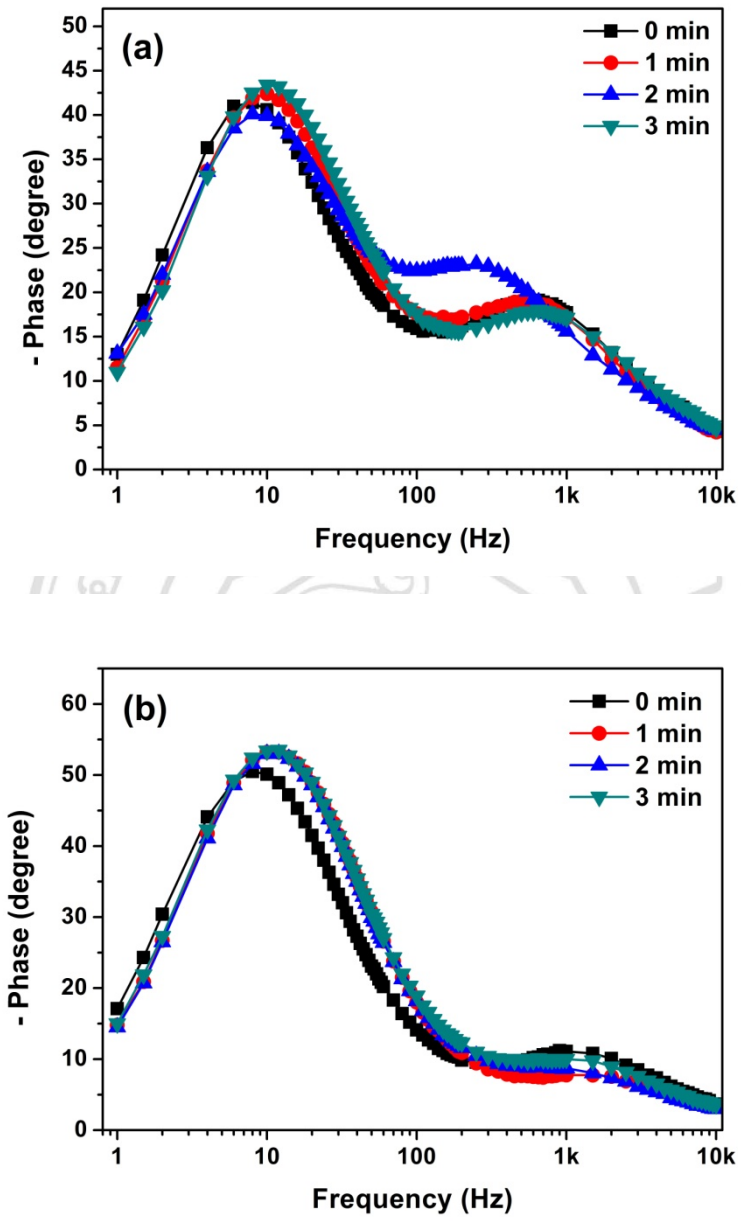

Figure 2.10 Bode phase plots of DSSCs fabricated with base texturing films for (a) EY sensitizer and (b) N719 sensitizer.

2.1.7 Effects of acid solution on photovoltaic performance

To understand the effects of texturing solution on photovoltaic performance, the acid solution was used to modify ZnO films for texturing time of 10, 20 and 30 s compare to the base solution. The J-V characteristics of N719 sensitized fabricated cells are shown in Figure 2.11, and photovoltaic parameters are listed in Table 2.5. It is found that J_{sc} shows small increase for texturing time of 10 s, but a significant decrease in J_{sc} is observed for texturing time over 10 s. The decreased J_{sc} indicates a reduction of dye adsorption. The reduced dye adsorption can be described by a rapid texturing process due to a strong chemical reaction of acid solution which might be not a good for improving an appropriate porous structure.

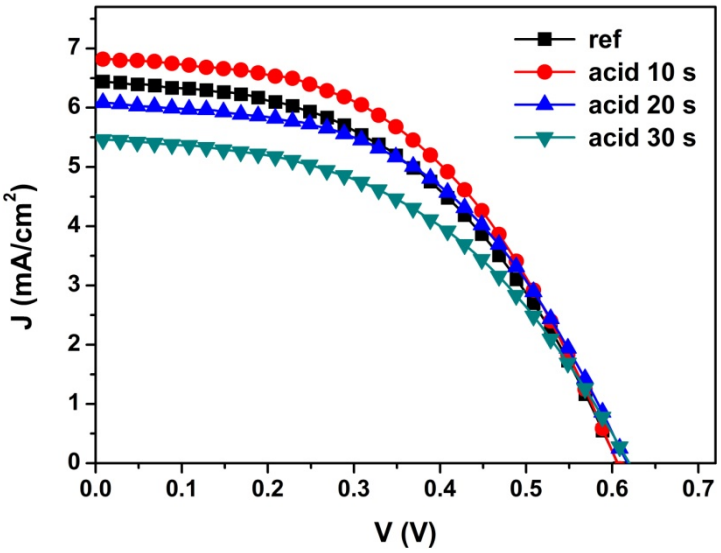

Figure 2.11 Photovoltaic characteristics of DSSCs fabricated with acid texturing films.

Table 2.5 Photovoltaic parameters of DSSCs fabricated with acid texturing films.

Texturing time (s)	J_{sc} (mA/cm^2)	V_{oc} (V)	FF	PCE (%)
0	6.43 ± 0.05	0.60 ± 0.01	0.48 ± 0.02	1.85 ± 0.08
10	6.82 ± 0.14	0.60 ± 0.01	0.50 ± 0.02	2.02 ± 0.01
20	6.09 ± 0.11	0.61 ± 0.01	0.50 ± 0.01	1.87 ± 0.01
30	5.47 ± 0.10	0.62 ± 0.01	0.48 ± 0.02	1.60 ± 0.07

Figure 2.12 showed a texturing ZnO surface by acid solution for texturing time of 10 s. The surface is smoother than the conventional screened ZnO films (see Figure 1.1(a)), and small pore is observed. In addition, simulated 3D profiles were analyzed by image-J software to investigate a fine porous formation [58]. The ordinary FE-SEM images were converted as gray scale with 8-bits (image >> type >> 8-bit), then analyzing the 3D profile (analyze >> 3D surface plot) as shown in Figure 2.13. The simulated 3D profiles show a good formation of fine porous structure which can be seen a better distributed peak and trough. The peak and trough of the texturing films show better valley-like structure than the conventional films indicating higher formation of porous structure. Moreover, the simulated roughness of the texturing films decreases to 102.94 nm compare to conventional films of 122.75 nm. The result confirms a formation of fine porous structure after the acid texturing process because aggregate particles are removed.

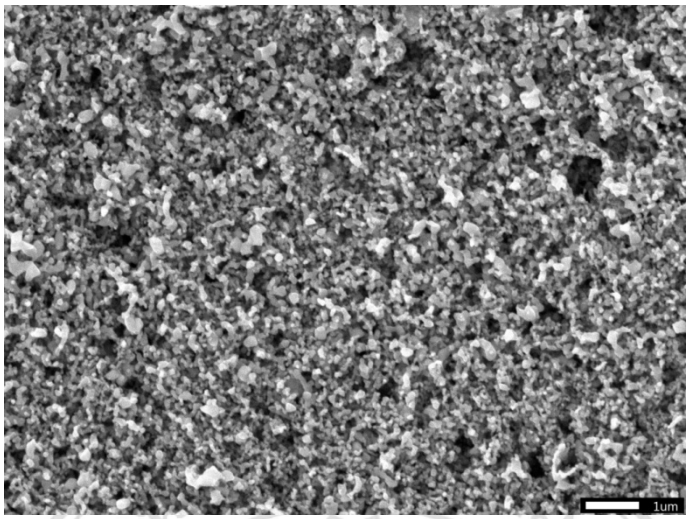

Figure 2.12 Morphology of acid texturing films for texturing time of 10 s.

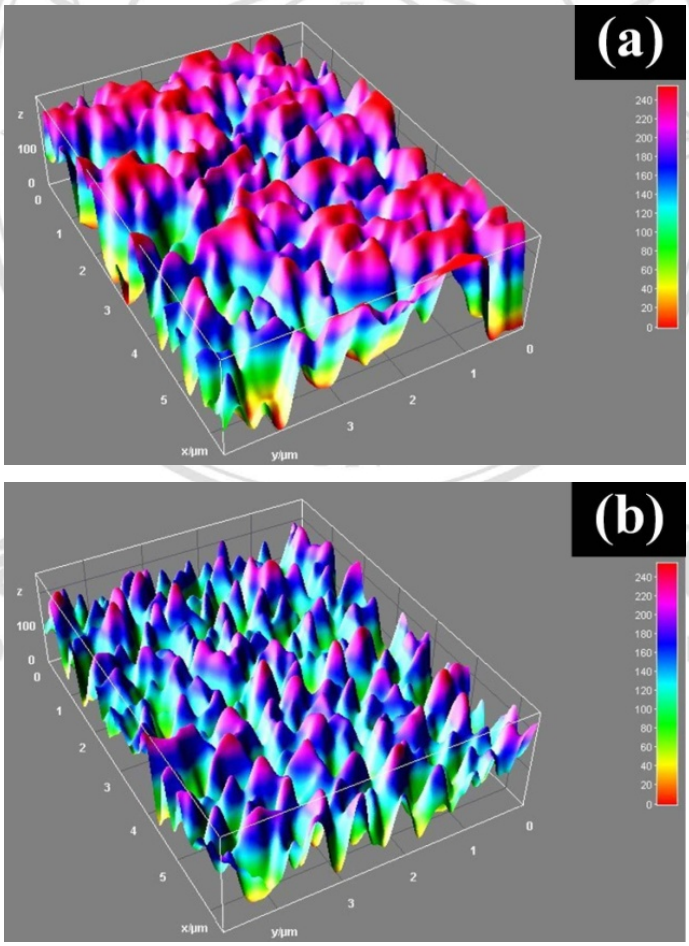

Figure 2.13 Simulated 3D profiles of (a) conventional screened ZnO films and (b) acid texturing ZnO films for texturing time of 10 s.

2.2 Two-step texturing process

Rough surface photoelectrodes with improved light scatting is presented using a two-step texturing process [71]. The Ti foil is treated with HF-KOH to create micro/nano structure for using as photoelectrodes in DSSCs. PCE is enhanced with a directly related to an increased J_{sc}. It is a result from an incident photon to current efficiency (IPCE) improvement which caused by the improved light scatting. A strategy in an increase of specific surface area is demonstrated using KOH solution texturing ZnO nanorods [34]. A decrease in diameter of nanorods is observed with the increased specific surface area. A fabricated DSSCs show an enhanced PCE over two times than a non-texturing ZnO nanorods photoelectrodes.

In this section, a two-step texturing process is used to texture ZnO films using sequential texturing step of base and acid solutions. For DSSCs application, J_{sc} and V_{oc} are expected to improve with an optimized film. Experimental samples were separated in two types as shown in Figure 2.14. Type I, ZnO films were firstly immersed in the base solution. After the rinsed and annealed, the films were repeating immersion in the acid solution followed by the rinsing and annealing process. For type II, the films were alternatively immersed in the acid solution and repeating immersed in the base solution. A texturing time is fixed of 10 s for acid solution and varied of 1-3 min for base solution.

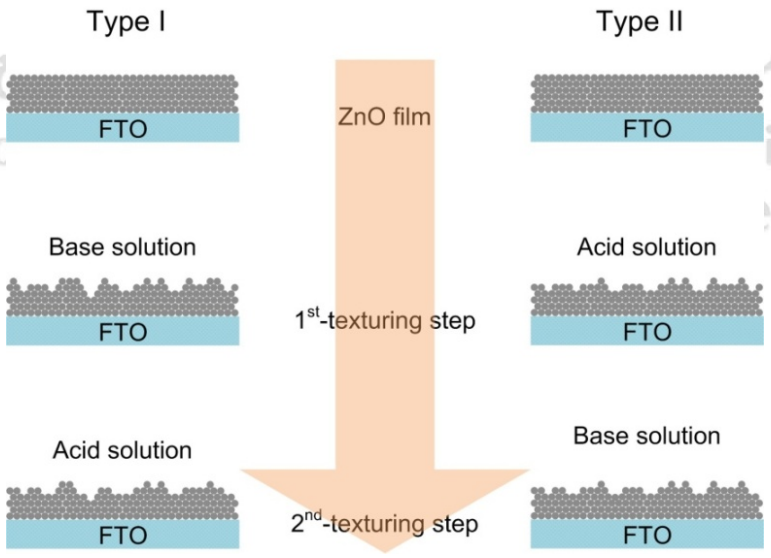

Figure 2.14 Schematic flow of a two-step texturing process.

2.2.1 Morphology

Figure 2.15 shows morphologies of type I films. It is found that the surface morphologies were not significant differences. A smooth zone, porous zone and crater-like zone were observed for all condition which is similar to the surface of type II as shown in Figure 2.16. Thus, there is not significant change in surface for both of type I and type II. However, the morphology of both types for two-step texturing films show a smoother porous structure than the one-step texturing films (see Figure 2.1). This result indicates a potential creation of smooth porous structure using combination of base and acid solutions.

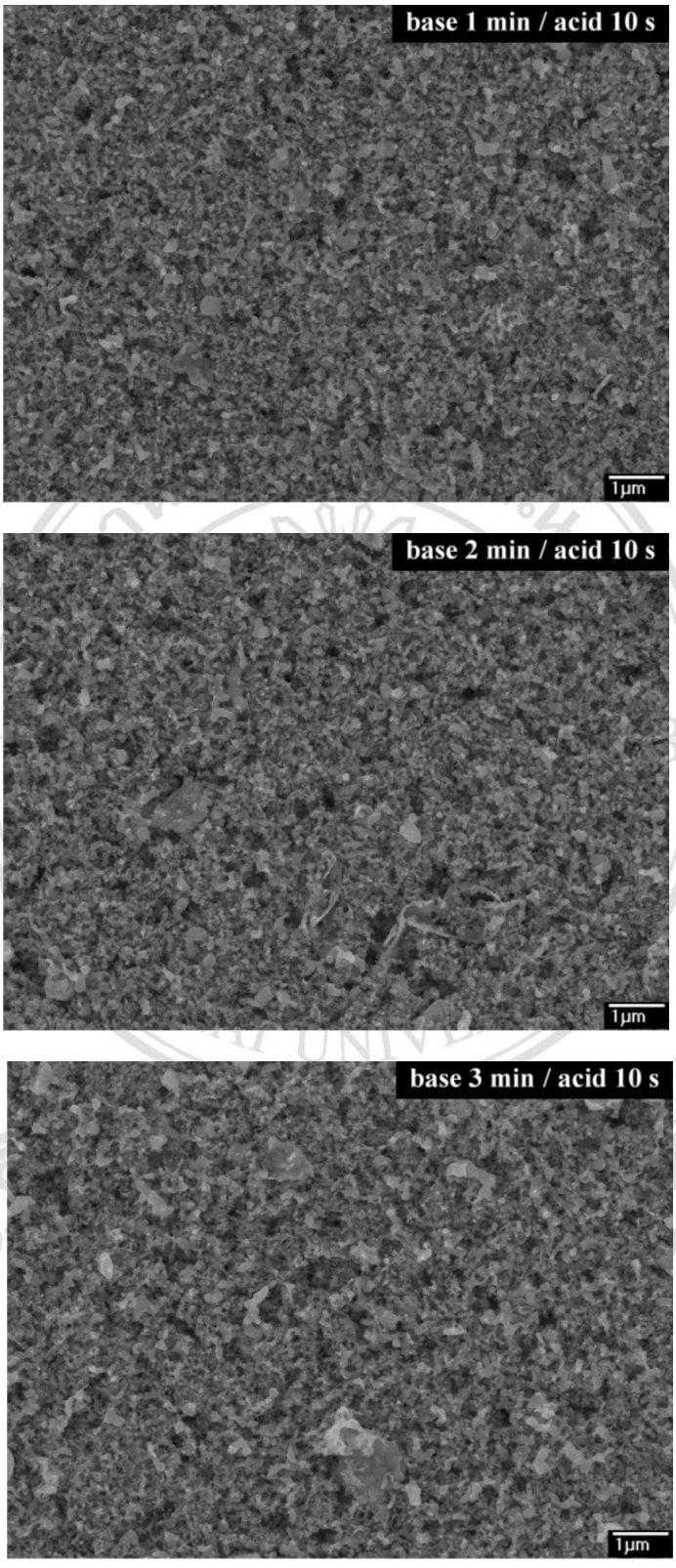

Figure 2.15 FE-SEM images of two-step texturing films for type I.

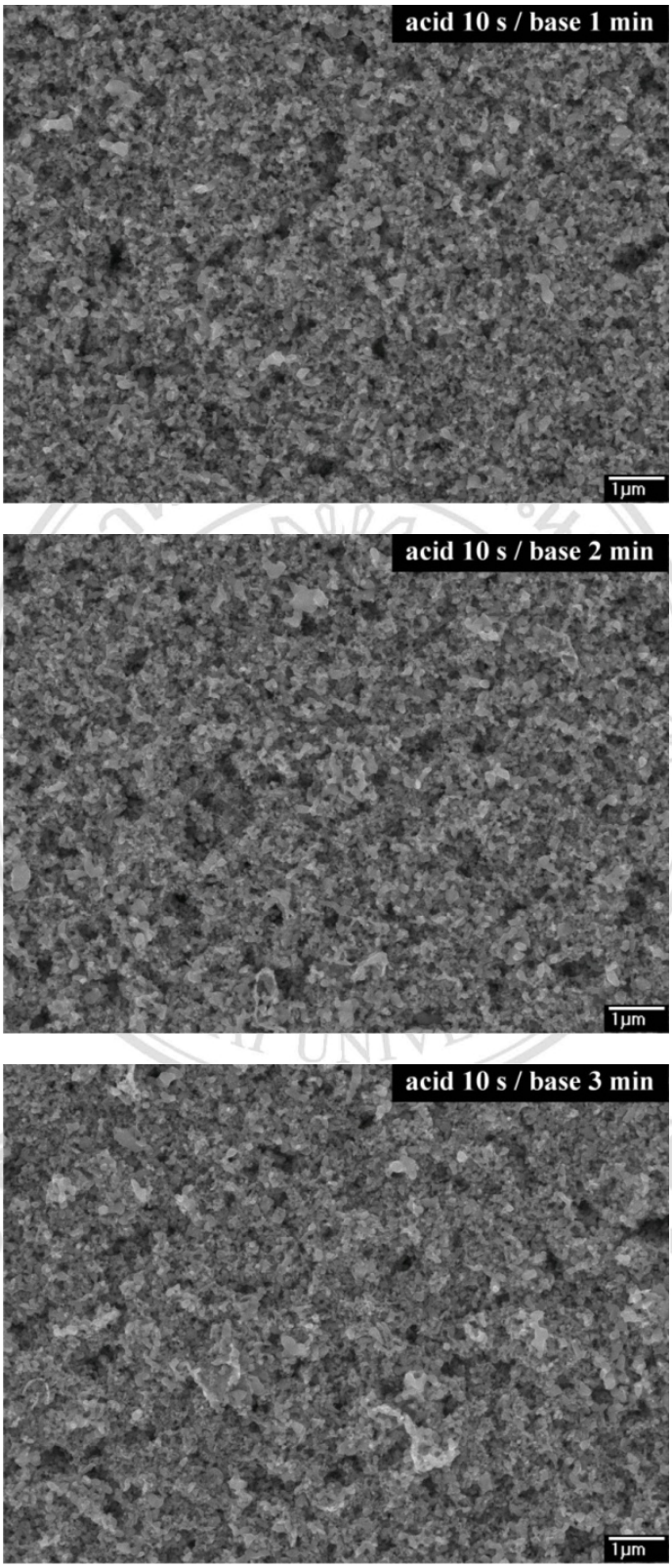

Figure 2.16 FE-SEM images of two-step texturing films for type II.

2.2.2 Simulated 3D profile analysis

Figure 2.17 and 2.18 show simulated 3D profiles of texturing ZnO films for both of type I and II, respectively. It is found that the type I texturing by base solutions for texturing time of 3 min and repeating texturing by acid solutions shows a wide range (green-blue scale) of peak and trough. A lower trough is appeared because chemical solutions penetrate into a deeper layer of ZnO films and remove the particles from the surface for long texturing time. This condition leads a deformation of porous structure and forms a crater-like structure. On the other hand, better smooth texturing films are observed for base solution texturing time of 1 and 2 min which can be seen that peak and trough are in the same range (green scale). Moreover, the texturing films with base solution for 2 min show an appropriate porous formation according to the better distribution of peak and trough. For type II, the 3D profiles show wide range (green-blue) for all conditions indicating that rough porous structure is formed after the secondary texturing by base solution.

These results suggest that the surface morphology of ZnO films can be modified by two-step texturing process using a sequential texturing solution of base and acid, respectively, and the second-step plays a key role to form a fine or rough porous structure. The observing rough and fine porous structures are formed after the second-step texturing by base and acid solutions, respectively. The appropriate fine porous films can be easily explained step by step of base and acid solutions. The first-step, base solution is used to texture the ZnO surface for creating rough porous structure. After the base texturing process, acid solution is used to repeating texture the films which is result to a fine porous structure creation in the second-step. Therefore, an appropriate fine porous structure is formed via a suiTable step of texturing solution.

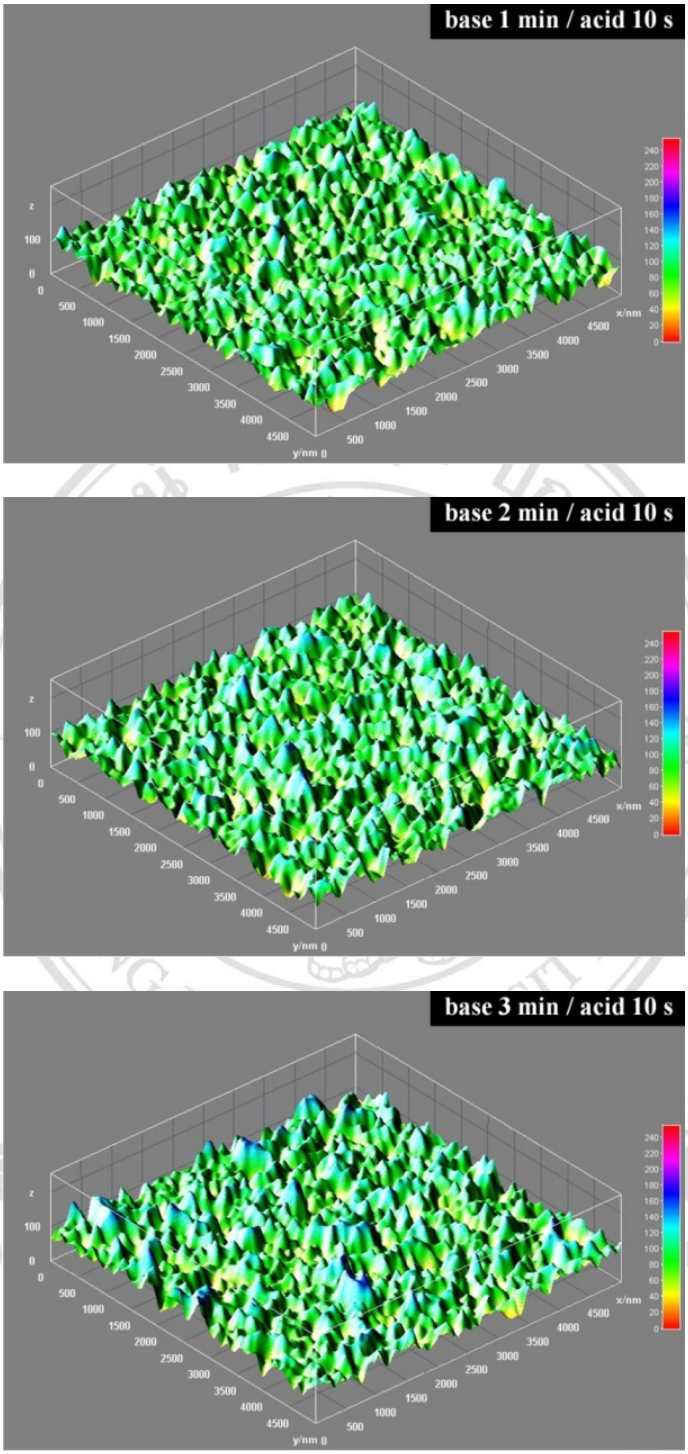

Figure 2.17 Simulated 3D profiles of two-step texturing films for type I.

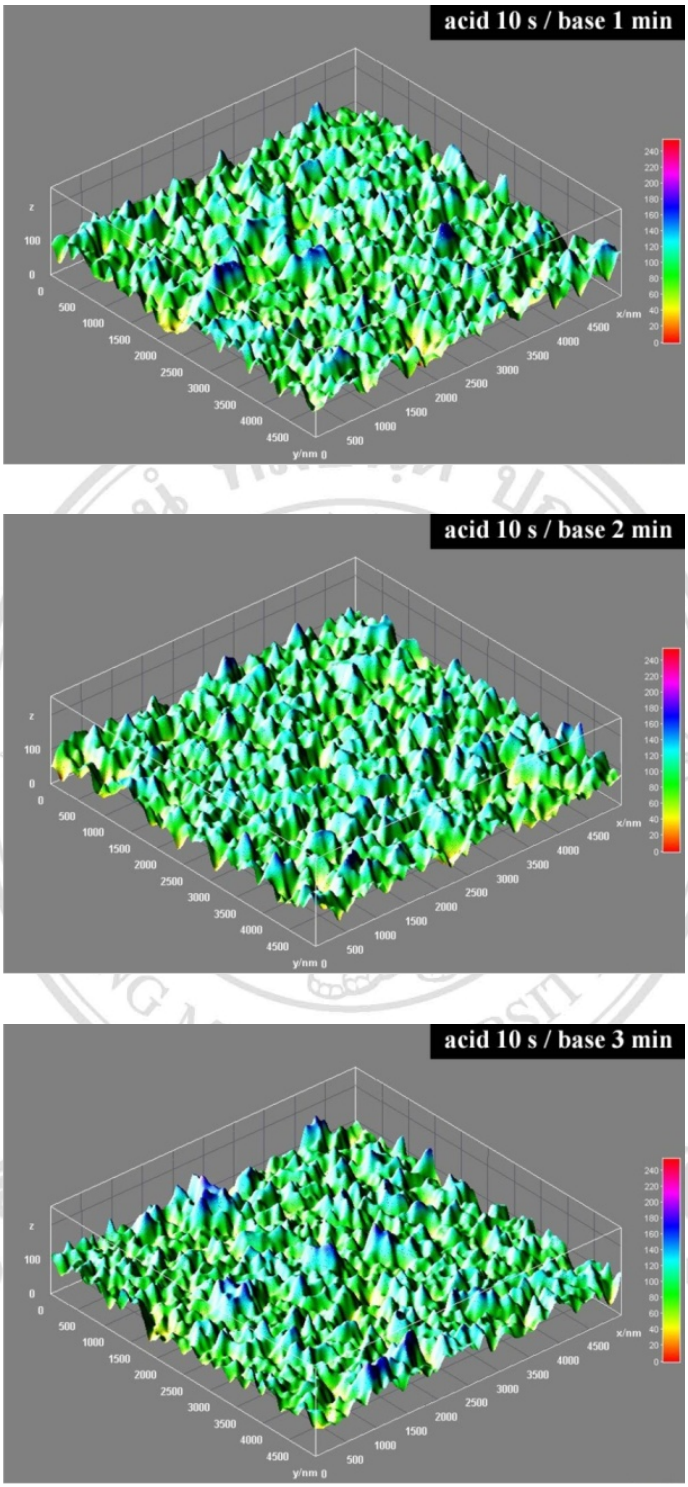

Figure 2.18 Simulated 3D profiles of two-step texturing films for type II.

2.2.3 Photovoltaic characteristics

To evaluate the two-step texturing films, all of the films were used as photoelectrodes for DSSCs application. The measured J-V characteristics are shown in Figure 2.19, and photovoltaic parameters are listed in Table 2.6.

For type I, J_{sc} shows slightly increase as increasing base solution texturing time while V_{oc} is still constant. PCE and FF are slightly increased and reached maximum values of 2.26 ± 0.01% and 0.52 ± 0.01, respectively, for base solutions texturing time of 2 min. In addition, the PCE and FF decrease in rapidly for base solutions texturing time of 3 min. The decrease confirms that the texturing time of 2 min is the optimal condition for type I. These result indicating that texturing step of base solution and repeating texturing by acid solution affects on the increase of J_{sc} and FF. The increased J_{sc} is due to better dye adsorption supported by fine porous structure. Moreover, the fine porous structure achieves better interfacial contact in the DSSCs and result the increase of FF.

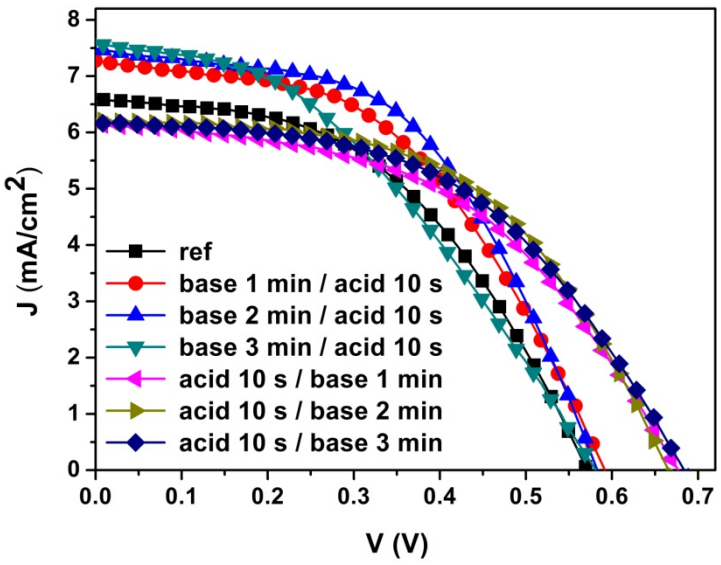

Figure 2.19 J-V characteristics of DSSCs fabricated with two-step texturing films.

Table 2.6: Photovoltaic parameters of DSSCs fabricated with two-step texturing films.

Texturing films	J_{sc} (mA/cm^2)	V_{oc} (V)	FF	PCE (%)
ref	6.61 ± 0.26	0.57 ± 0.01	0.48 ± 0.02	1.80 ± 0.01
base 1 min / acid 10 s	7.26 ± 0.04	0.59 ± 0.01	0.49 ± 0.01	2.09 ± 0.01
base 2 min / acid 10 s	7.49 ± 0.05	0.58 ± 0.01	0.52 ± 0.01	2.26 ± 0.01
base 3 min / acid 10 s	7.56 ± 0.12	0.58 ± 0.01	0.41 ± 0.01	1.77 ± 0.04
acid 10 s / base 1 min	6.15 ± 0.11	0.67 ± 0.01	0.49 ± 0.01	2.04 ± 0.01
acid 10 s / base 2 min	6.23 ± 0.08	0.66 ± 0.01	0.54 ± 0.01	2.20 ± 0.01
acid 10 s / base 3 min	6.17 ± 0.06	0.68 ± 0.01	0.51 ± 0.01	2.13 ± 0.01

For type II, PCE shows slightly increased and reached maximum value of 2.20 ± 0.01% for base solution texturing time of 2 min consistent with the trend of FF, while J_{sc} is decreased. However, V_{oc} exhibit a significant increase similar to the one-step texturing films by acid solution. The results suggesting that the texturing step of acid solution and repeating texturing by base solution affects on the increase of V_{oc} and FF. The increase of V_{oc} might be due to an improved interface contact [72]. A direct interface contact between ZnO and electrolyte is increased as increasing porous structure. The type II might be better in porous structure than the type I because the 1^{st}-texturing step by acid solution can better removes aggregate particles in the bottom films with a rapid reaction compare to base solution texturing. Thus, the extended V_{oc} is due to the improved direct interface contact of ZnO/electrolyte.

It is seen that J_{sc} and V_{oc} exhibit much differences for both types. The type I displays a higher J_{sc} than both of type II and the reference. This effect can be described as the formation of an appropriate fine porous structure. In addition, the increase of J_{sc}

shows a similar trend with the one-step texturing films by base solution. It is observed that the effects of the 1st-texturing step by base solution show more dominating effect than the 2nd-texuring step by acid solution. On the other hand, the type II shows higher V_{oc} because interface contact is improved. These results suggest that the texturing process of base and acid solutions can improve J_{sc} and V_{oc}, respectively. In addition, the increase of V_{oc} shows similar trend with the one-step texturing films by acid solution.

To compare the performance of DSSCs fabricated two-step texturing films and one-step texturing films, the fabricated cells with maximum PCE were selected as an optimal samples for each processes; (i) base texturing films for texturing time of 2 min was selected as a sample of one-step texturing films, (ii) texturing films with sequential texturing step of base solution for texturing time of 2 min and repeating texturing by acid solution for texturing time of 10 s was selected as a sample of two-step texturing films, (iii) and non-texturing films was used as a reference for comparing performance as shown in Figure 2.20. According to the photovoltaic parameters, the V_{oc} of DSSCs fabricated on two-step texturing films, one-step texturing films and non-texturing films show not significant differences. The result indicates a stability of internal crystal structure, thus the solutions have no potential to change fundamental crystal. On the other hand, J_{sc} and FF of both modified films show a significant increase in comparison to the non-texturing films. Moreover, the maximum DSSCs performance is observed for the two-step texturing films based DSSCs. This result imply that fine porous structure support better dye adsorption and interface contact of ZnO/Dye/electrolyte providing better electron generation and redox process in the DSSCs, respectively. Therefore, the two-step texturing process was demonstrated an interesting surface modification method that can be used to texture ZnO films for enhancing high DSSCs performance.

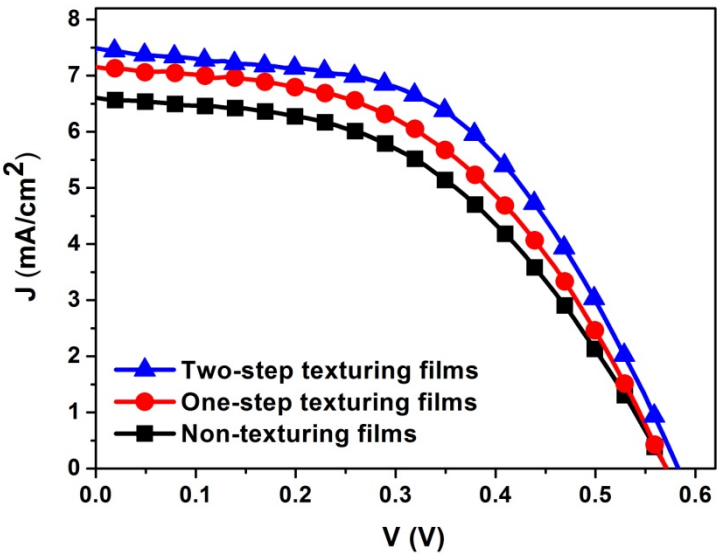

Figure 2.20 J-V characteristics of DSSCs fabricated with optimal two-step texturing films, one-step texturing films and non-texturing films.

2.2.4 Pore analysis

To clearly understand the effect of texturing process on surface change, the texturing films were investigated. An image processing technique using image-J software is used for analyzing the pore size distribution of two-steps texturing film, one-step texturing films and non-texturing films for each optimization. For processing details, ordinary FE-SEM images were converted as gray scale with 8-bits (image >> type >> 8-bit), threshold adjustment (image >> adjust >> threshold >> auto), then analyzing the pore size (analyze >> analyze particles). Figure 2.21 show pore size distribution, all of the samples are in similar trends. A dominating pore size is appeared in range of 5-10 nm, and pore count frequency shows a significant higher than that another ranges. Moreover, the maximum count frequency is observed for the two-step texturing films agreed with a maximum specific surface area. The measured specific surface area of two-step texturing films show a significantly increase to 7.07 m^2/g compared with one-step texturing films (5.30 m^2/g) and non-texturing films (2.52 m^2/g). This result confirms a fine porous ZnO films prepared by using two-step texturing process provide a high specific surface area for achieving dye adsorption.

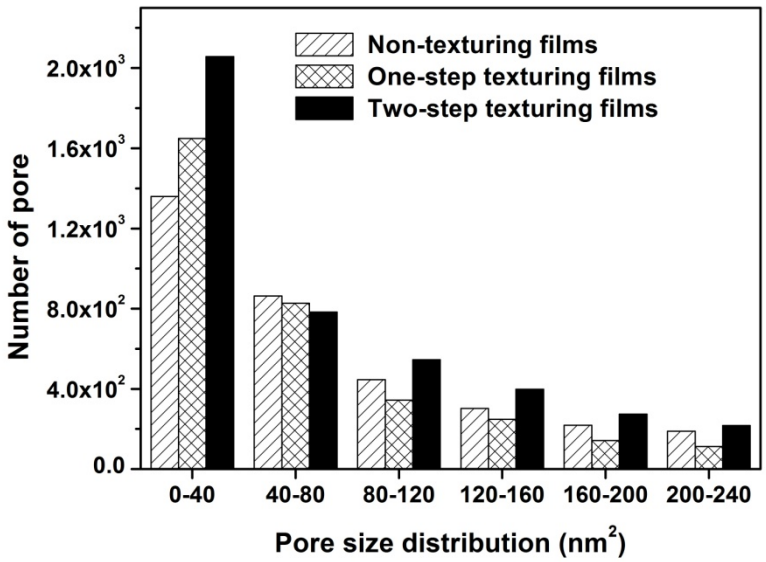

Figure 2.21 Pore size distribution of non-texturing films, one-step texturing films and two-step texturing films.

2.2.5 Raman shift

Raman shift was measured as shown in Figure 2.22. The Raman shift intensity decrease after texturing due to decreased thickness and the formation of porous structure. However, the Raman shift is not changed for all major peaks indicating that there are no leaving species (such as O vacancies) on the texturing films after the texturing process. Therefore, this result confirms that the chemical corrosion is a major key for forming fine porous structure.

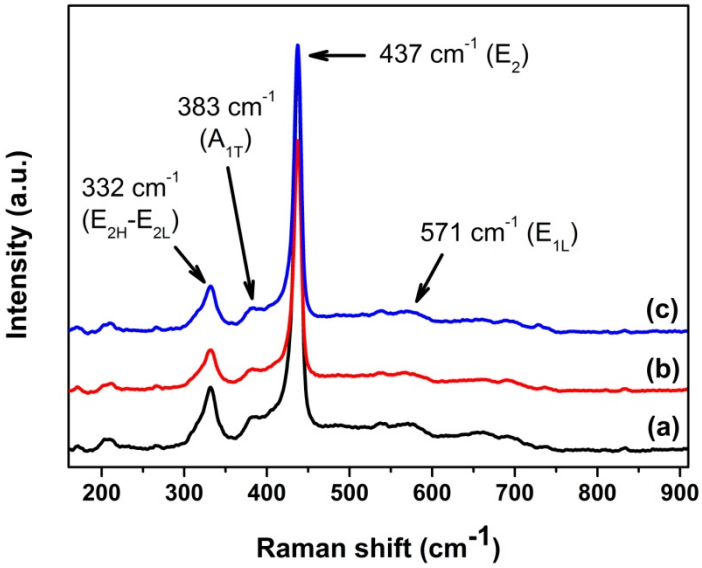

Figure 2.22 Raman shift of (a) non-texturing films, (b) one-step texturing films and (c) two-step texturing films.

2.3 Surface modification of Pt counterelectrodes

After Pt counterelectrode was prepared, it was textured by immersed into the mixed acid solution for 10 s, washed and heated at 120 ^{o}C for 30 min. After heating, the Pt counterelectrode was used in DSSCs to evaluate cell performance. Morphology was observed by SEM and analyzed by image-J software. Reflectance was measured by UV-Vis NIR spectroscopy.

2.3.1 Morphology

Figure 2.23 shows morphologies of non- texturing and texturing Pt films. The observed surface morphologies were not significant differences. Pt films formed particle-like. Relative surface roughness of the non-texturing films was 116.06 nm and increased as 128.17 nm after texturing. The result indicated that Pt particles were removed from surface to form rough films.

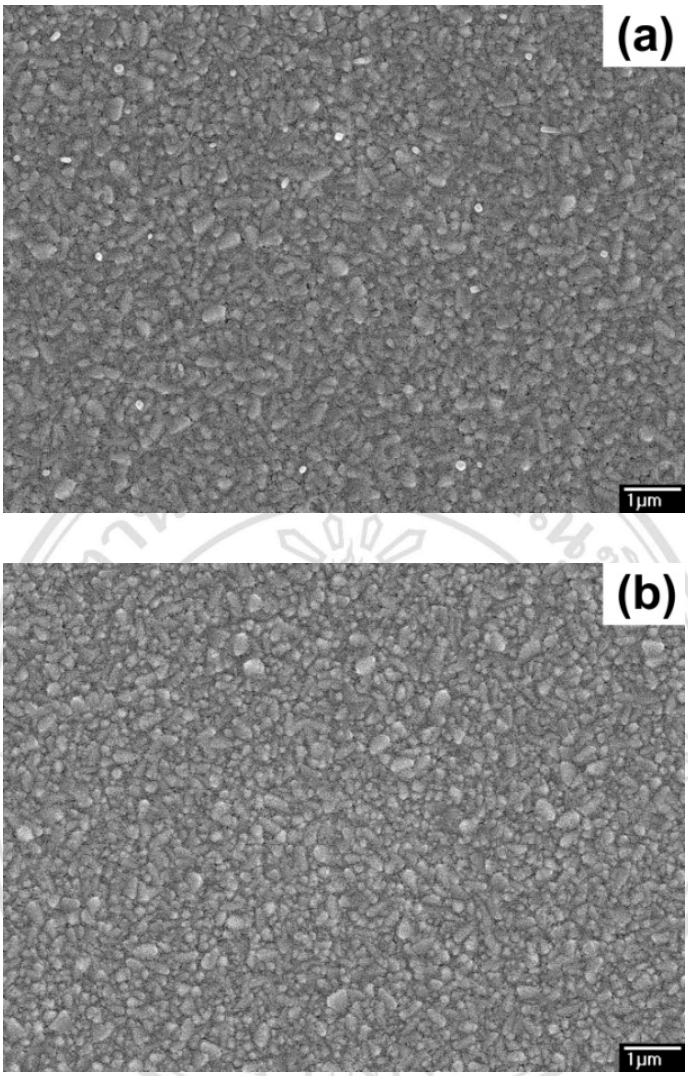

Figure 2.23 SEM images of (a) non-texturing Pt films and (b) texturing Pt films.

2.3.2 Reflectance

Surface reflectance of Pt counterelectrodes with and without acid texturing was shown in figure 2.24. The observed reflectance decreased after texturing with average reflectance in visible region (400-700 nm) of 4.31% and 3.32% for non-texturing and texturing Pt films, respectively. The result agreed with the increase of relative roughness that supports more scattering.

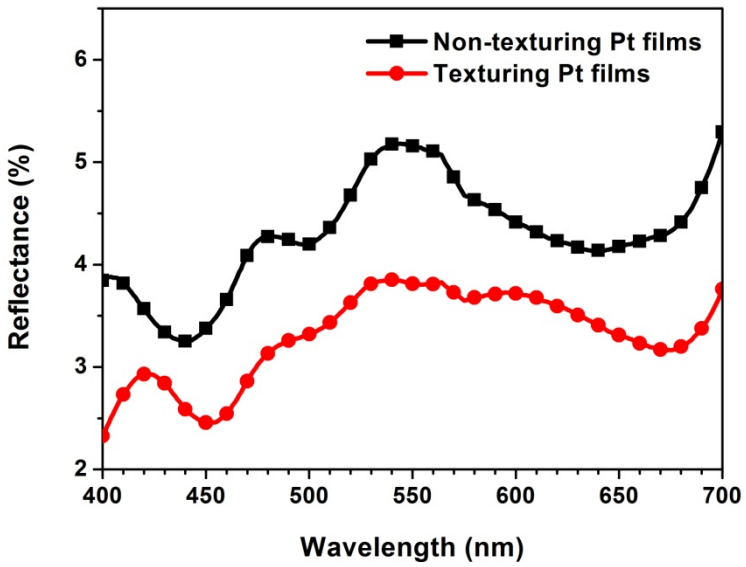

Figure 2.24 Reflectance of non-texturing and texturing Pt films.

2.3.3 Photovoltaic characteristics

J-V characteristics of DSSCs fabricated with non-texturing and texturing Pt films showed insignificant difference as shown in figure 2.25. The J-V characteristics were insignificantly observed for both films. In addition, parameters were listed in table 2.7. J_{sc} showed a small increased might be due to an increased surface area of the texturing Pt films. However, DSSCs performance is indifference compared with the non-texturing films based. It can be interpreted that texturing Pt films with acid solution have no significance for improving DSSCs performance. Therefore, surface modification of Pt counterelectrode is not considered in the next chapter, and only non-texturing Pt films are used for investigating more significant surface modification of ZnO photoelectrodes.

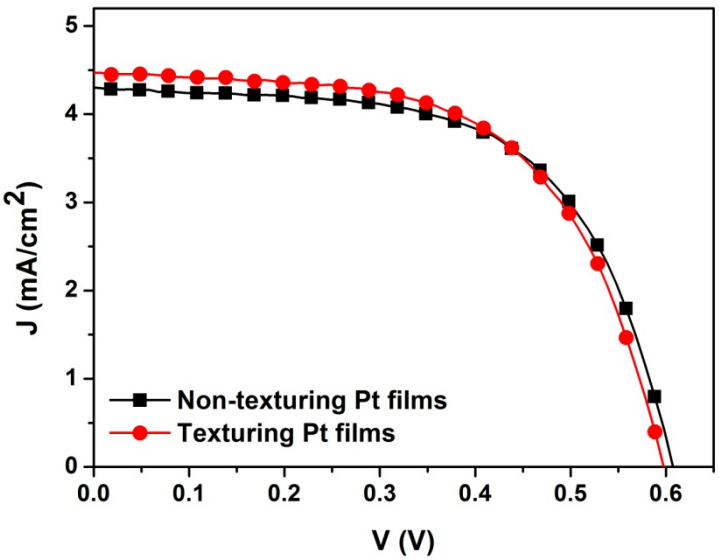

Figure 2.25 J-V characteristics of DSSCs fabricated with non-texturing and texturing Pt films.

Table 2.7: Photovoltaic parameters of DSSCs fabricated with non-texturing and texturing Pt films.

Counterelectrode films	**J_{sc} (mA/cm^2)**	**V_{oc} (V)**	**FF**	**PCE (%)**
Non-texturing Pt film	4.30 ± 0.04	0.60 ± 0.01	0.61 ± 0.01	1.59 ± 0.02
Texturing Pt film	4.47 ± 0.03	0.59 ± 0.01	0.60 ± 0.01	1.59 ± 0.01

2.3 Summary of chemical wet texturing process

One-step texturing films using base and acid solutions show the optimal texturing time of 2 min and 10 s, respectively. The base and acid solutions have the roles for improving rough and fine porous structured films which is an important structure for better dye adsorption. N719-sensitized DSSCs fabricated on base and acid texturing films exhibit enhanced power conversion efficiency of 2.00% and 2.02%, respectively,

which is higher than a conventional films of 1.85%. Two-step texturing films demonstrate a better high-ordered fine porous structure than that of the one-step texturing films. The improved fine porous structure is observed by a significant increase for small pore size in range of 5-10 nm and confirmed by maximum specific surface area. It is considerate an important factor for achieving dye adsorption and enhancing power conversion efficiency to 2.26%. The result demonstrate a potentiality of two-step texturing process using sequential texturing step of base and acid solutions for surface modification of ZnO films. For the surface modification of Pt counterelectrode, it can be concluded that Pt counterelectrode texture by chemical texturing process with acid solution is not significance for enhancing power conversion efficiency of DSSCs. Therefore, the texturing Pt films are excluded in next chapter and only surface modification of photoelectrodeds is mentioned. The non-texturing Pt films are used for all devices in next chapter to focus on surface modification technique of ZnO photoelectrodes.